Wave-Coherent Fields in Air Flow over Ocean Waves: Identification of Cooperative Behavior Buried in Turbulence

Tihomir Hristov,* Carl Friehe, and Scott Miller

Department of Mechanical and Aerospace Engineering, University of California, Irvine, California 92697-3975

(Received 29 June 1998)

We present a method to study the coupling and synchronization of two chaotic systems—the surface gravity waves in the open ocean and the turbulent air flow above. Our approach employs an eikonal-like representation of the wave field based on the concept of an analytic signal and the Hilbert transform. We identify a wave-coherent component in the air flow which is phase locked with the waves and deeply buried in turbulence. That component contributes most of the wind-wave energy and momentum exchange, so its identification from actual data is of primary interest. We define and obtain the phase shifts of the wave-coherent fields and discuss their roles in the wind wave exchange. [S0031-9007(98)07829-6]

PACS numbers: 92.10.Hm, 47.27.Eq, 47.35.+i, 47.52.+j

Cooperative behavior plays a major role in a variety of chaotic systems, but it may be hard to identify and quantify. A good example is the coupling between ocean surface waves (which are not periodic) and the randomly fluctuating turbulent wind above, where a small (relative to the turbulent fluctuations) wave-coherent component in the wind is believed to carry most of the wind-wave interaction. Today's climate and weather forecasting models are built on assumptions (many of which are untested experimentally, [1]) about the mechanisms and intensity of the exchange of kinetic energy and momentum between the ocean and the atmosphere. In spite of decades-long efforts, starting from Jeffreys in 1924 [2], expanded by Miles [3] and Phillips [4], and recent advances in [5,6], current knowledge regarding wind-wave interactions is limited due to experimental and theoretical difficulties [1,7,8]. The wide inconsistency among the experimental estimates for the wind-wave energy exchange [8], possibly amplified by the lack of technique to extract the wave-coherent component in the air flow, as well as the absence of field data for the wave-induced Reynolds stresses (which impedes the closure modeling) are some of those difficulties. Laboratory experiments on wind-wave coupling do not reproduce the scales and conditions over the open ocean [9], so the field experiments remain as relevant and necessary components of this research. In this study we use data from the marine boundary layers experiment, which took place 50 kilometers off the coast of California on the stable floating instrument platform (FLIP). The instruments were positioned at fixed heights from 2.7 to 18.1 m above the interface and the wave height was registered directly beneath them.

Intuitively, one might expect that the fluctuations of velocity and pressure in the air flow over waves are of two kinds, originating either from the shear-driven turbulence, or induced by the underlying waves. Assuming that the two kinds of fluctuations are weakly coupled, the flow velocity $\mathbf{u} \equiv (u, v, w)$ and pressure p can be decomposed into mean, turbulent, and wave-induced components, $\mathbf{u} = \overline{\mathbf{u}} + \mathbf{u}' + \tilde{\mathbf{u}}$ and $p = \overline{p} + p' + \tilde{p}$. The turbulent pressure fluctuations p' can lead to wave growth through a random walk process [4], but their contribution appears to be too small to explain the observed growth rates [7]. The wave-induced component $\{\tilde{\mathbf{u}}, \tilde{p}\}$ is predicted to produce the major contribution to the short waves growth through a resonant mechanism of shear-flow instability [3]. In this mechanism the waves modify the air flow by phase shifting the mean flow streamlines (cat's-eye pattern, [10]) and induce velocity and pressure fluctuations phase locked with the waves. Thus, the component $\{\tilde{\mathbf{u}}, \tilde{p}\}$ carries and embodies the cooperative behavior in the wind-wave system. Synchronization between driving and driven subsystems is known to be possible when the driven subsystem is more stable than the driving system [11], as in the wind(driving)-wave(driven) case. Further understanding of wind-wave coupling requires the identification of $\{\tilde{\mathbf{u}}, \tilde{p}\}$ in field-experiment data by separating it from the turbulent component $\{\mathbf{u}', p'\}$. The problem of separation of $\{\tilde{\mathbf{u}}, \tilde{p}\}$ and $\{\mathbf{u}', p'\}$ is difficult [12,13] and unsolved. Since the spatial and time scales of $\{\tilde{\mathbf{u}}, \tilde{p}\}$ and $\{\mathbf{u}', p'\}$ overlap, Wiener filtering is not applicable. In this Letter, we propose a method which produces optimal estimates for the wave-induced component in the wind.

An approach to the decomposition problem is to assume that the turbulent and the wave coherent components in the air flow are not correlated and are statistically stationary. Let us consider monochromatic waves with a period T_0 and the air velocity $\mathbf{u}$ at a fixed height above the mean ocean surface. Under these assumptions, the synchronized average of the air velocity for an interval of length $(2N + 1)T_0$ defined as

$$\hat{S}\mathbf{u}(t) \stackrel{\text{def}}{=} \left(\frac{1}{2N + 1} \sum_{n=-N}^{N} \mathbf{u}(t + nT_0) \right) - \overline{\mathbf{u}} \qquad (1)$$

should filter out the turbulence and leave the phase average of the wave-coherent component $\tilde{\mathbf{u}}(t)$. In lab experiments with monochromatic waves [8], this technique should perform well. However, the waves in the open

ocean are continuously spread over an interval of spectral scales. Taking T_0 equal to the period T_p of the most energetic (peak) mode in the wave spectrum and using (1) with field data leads to a strong attenuation of $\hat{S}\mathbf{u}(t)$ as a result of the destructive interference of multiple modes. This obstacle is encountered by attempts to use $\hat{S}$ to separate $\{\mathbf{u}', p'\}$ and $\{\tilde{\mathbf{u}}, \tilde{p}\}$, and motivated the development of an approach which would be more robust—i.e., far less sensitive to the lack of coherence in nonmonochromatic wave fields. The approach we explore and later apply uses nonlinear filtering and is based on an eikonal-like representation of the wave signal.

To introduce the idea, let us recall that a signal consisting of two Fourier components $A_1 e^{i\omega_1 t}$ and $A_2 e^{i\omega_2 t}$ has instantaneous amplitude $A(t)$ and phase $\varphi(t)$ formed by the rule $A(t)e^{i\varphi(t)} = A_1 e^{i\omega_1 t} + A_2 e^{i\omega_2 t}$. For a signal of an arbitrary spectrum $s(t)$, the idea can be generalized by employing the concept of an analytic signal based on the Hilbert transform [14]. The analytic signal $\Psi(t)$ is a complex-valued function of time defined as

$$\Psi(t) = s(t) + i\hat{\mathcal{H}}s(t) = A(t)e^{i\Phi(t)}, \tag{2}$$

where $\hat{\mathcal{H}}s(t)$ is the Hilbert transform of $s(t)$

$$\hat{\mathcal{H}}s(t) \stackrel{\text{def}}{=} \frac{1}{\pi}\,\text{P.V.}\int_{-\infty}^{\infty}\frac{s(\tau)}{t-\tau}\,d\tau\,, \tag{3}$$

and P.V. indicates that the integral is taken in the sense of a Cauchy principal value. Thus, (2) uniquely determines the instantaneous amplitude $A(t)$ and the instantaneous phase $\Phi(t) = \text{Arg}[s(t) + i\hat{\mathcal{H}}s(t)]$ of the signal $s(t)$. From (3), the Hilbert transform $\hat{\mathcal{H}}s(t)$ may be seen as the convolution of the functions $s(t)$ and $1/\pi t$. The Fourier transforms $S(\omega)$ of $s(t)$ and $S_{\hat{\mathcal{H}}}(\omega)$ of $\hat{\mathcal{H}}s(t)$ are related as $S_{\hat{\mathcal{H}}}(\omega) = -i\ \text{sgn}\,(\omega)S(\omega)$; i.e., the transform (3) preserves the amplitudes and introduces a constant $\pi/2$ lag at all positive frequencies [14].

Now we will define a filter to estimate the wave-coherent component $\{\tilde{\mathbf{u}}, \tilde{p}\}$. Let $\eta(t)$ be the wave height signal over a time interval $[-T, T]$ $(T \gg T_p)$ and let $\mathbf{u}(t)$ be the wind velocity vector at a fixed height above the mean ocean surface. Let $\Phi(t) = \text{Arg}[\eta(t) + i\hat{\mathcal{H}}\eta(t)]$ (phase modulo 2π) be the wave's instantaneous phase, as defined in (2). The filter should not cause destructive interference which makes $\hat{S}$ fail to separate $\{\tilde{\mathbf{u}}, \tilde{p}\}$ from $\{\mathbf{u}', p'\}$. For that purpose the filter should average the signal $\mathbf{u}(t)$ or $p(t)$ at the points in time where the wave phase is the same. Thus, the wave-coherent component $\tilde{\mathbf{u}}(t)$ can be estimated as a conditional expectation $E[\mathbf{u} - \overline{\mathbf{u}}\,|\,\Phi = \Phi(t)]$ of the wind velocity fluctuations $\mathbf{u} - \overline{\mathbf{u}}$ at all the moments of time τ when the wave phase $\Phi(\tau) = \Phi(t)$, by using the transform

$$\hat{\mathcal{P}}\mathbf{u}(t) \stackrel{\text{def}}{=} -\overline{\mathbf{u}} + \lim_{T\to\infty}\frac{\int_{-T}^{T}\mathbf{u}(\tau)\,|\Phi'(\tau)|\,\delta(\Phi(\tau)-\Phi(t))\,d\tau}{\int_{-T}^{T}|\Phi'(\tau)|\,\delta(\Phi(\tau)-\Phi(t))\,d\tau} \tag{4}$$

[analogously for $\hat{\mathcal{P}}p(t)$], where $\Phi'(\tau) \equiv d\Phi(\tau)/d\tau$. For monochromatic signals $\eta(t)$, (4) is equivalent to (1). For nonmonochromatic wave signals, $\hat{S}$ and $\hat{\mathcal{P}}$ show very different results (Fig. 1). Because of destructive interference, the averages $\hat{S}\eta(t)$ and $\hat{S}u(t)$ of 10 dominant wave periods ($T_p = 9s$) are attenuated and distorted [Fig. 1(c), 1(e)]. In contrast, $\hat{\mathcal{P}}\eta(t)$ and $\hat{\mathcal{P}}u(t)$ show almost no attenuation or distortion [Fig. 1(d), 1(f)].

Although $\hat{\mathcal{P}}$ can suppress the turbulence and emphasize the wave-coherent quantities, $\hat{\mathcal{P}}$ lacks some necessary properties. For instance, $\hat{\mathcal{P}}$ is insensitive to varying wave amplitude $A = |\eta + i\hat{\mathcal{H}}\eta|$ and if applied to the wave signal it does not reproduce it, i.e., $\hat{\mathcal{P}}\eta(t) \neq \eta(t)$. Therefore, the idea used in (4) should be extended to obtain an estimate for $\{\tilde{\mathbf{u}}, \tilde{p}\}$ as conditional expectations $\tilde{\mathbf{u}}(t) = E[\mathbf{u} - \overline{\mathbf{u}}\,|\,A = A(t), \Phi = \Phi(t)]$ and $\tilde{p}(t) = E[p - \overline{p}\,|\,A = A(t), \Phi = \Phi(t)]$ through the transform

$$\hat{\mathcal{N}}\mathbf{u}(t) \stackrel{\text{def}}{=} -\overline{\mathbf{u}} + \lim_{T\to\infty}\frac{\int_{-T}^{T}\mathbf{u}(\tau)\,|\Psi'(\tau)|\,\delta(\Psi(\tau)-\Psi(t))\,d\tau}{\int_{-T}^{T}|\Psi'(\tau)|\,\delta(\Psi(\tau)-\Psi(t))\,d\tau} \tag{5}$$

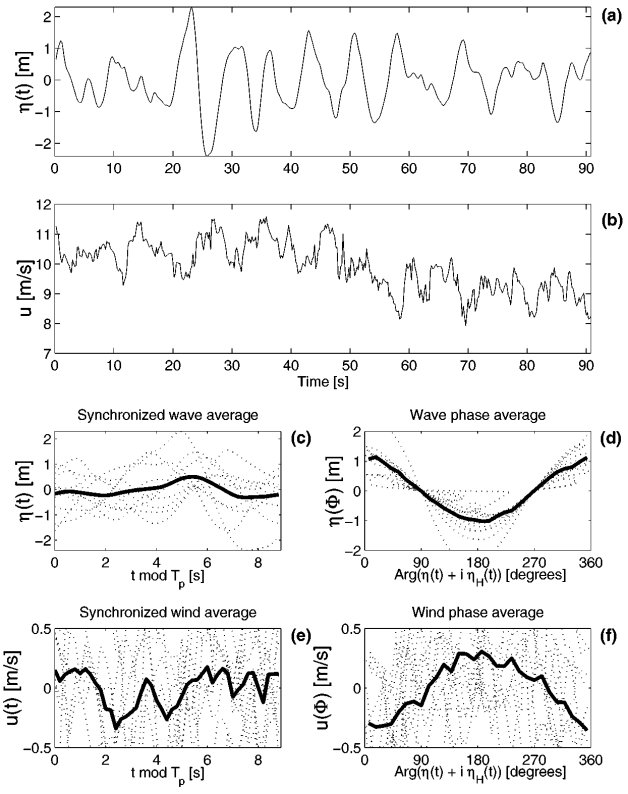

FIG. 1. (a) Wave height signal $\eta(t)$ vs time; (b) measured stream-wise wind velocity $u(t)$ vs time; (c) wave synchronized average $\hat{S}\eta(t)$; (d) wave phase average $\hat{\mathcal{P}}\eta(t)$; (e) wind synchronized average $\hat{S}u(t)$; (f) wind phase average $\hat{\mathcal{P}}u(t)$. T_p is the period of the most energetic wave mode. The dotted lines in (c) and (e) show $\eta(t)$ from (a) vs $t \bmod T_p$. The dotted lines in (d) and (f) show $u(t)$ from (b) vs Φ. The solid lines in (c), (d), (e), and (f) represent the synchronized or phase averages. For the interval shown in (a) and (b) the wind and waves are well aligned.

[analogously for $\hat{\mathcal{N}}p(t)$], where $\Psi(t) = \eta(t) + i\hat{\mathcal{H}}\eta(t) = A(t)e^{i\Phi(t)}$ and $\Psi'(\tau) \equiv d\Psi(\tau)/d\tau$. Let us note that: (i) $\hat{\mathcal{N}}$ reproduces the wave height, i.e., $\hat{\mathcal{N}}\eta(t) = \eta(t)$. (ii) $\hat{\mathcal{N}}(\cdot)$ as a conditional expectation $E((\cdot)\,|\,\Psi)$ expresses an orthogonal projection operator in a Hilbert space and thus is the optimal (in a least squares sense) estimator [15] for $\{\tilde{\mathbf{u}}, \tilde{p}\}$. As such, $\hat{\mathcal{N}}$ satisfies $\langle\hat{\mathcal{N}}\mathbf{u}(t), \eta(t)\rangle = \langle\mathbf{u}(t), \eta(t)\rangle$; i.e., $\hat{\mathcal{N}}\mathbf{u}(t)$ carries all the information about the coupling of the measured signal $\mathbf{u}(t)$ [or $p(t)$] with the wave $\eta(t)$, but has minimal energy (variance). (iii) $\hat{\mathcal{N}}$ is equivalent to $\hat{\mathcal{S}}$ for monochromatic waves $\eta(t)$. Consider the subspaces M_k, $k = 1, \ldots, N$ corresponding to finite width frequency subbands in the frequency range of the wave signal and let $\eta_k(t) = \mathrm{pr}_{M_k}\eta(t)$ be the projection of $\eta(t)$ onto M_k. The filtering $\hat{\mathcal{N}}$ can be performed in every one of these subspaces if preservation of the covariance in every subspace $\langle\tilde{\mathbf{u}}_k(t), \eta_k(t)\rangle = \langle\mathbf{u}_k(t), \eta_k(t)\rangle$ is needed. By using the preservation of the covariance in the subspaces (i.e., projection onto η_k in every subspace) as a criterion for separation of $\{\tilde{\mathbf{u}}, \tilde{p}\}$ and $\{\mathbf{u}', p'\}$, the design of a linear filter for that purpose is also possible

$$\hat{\mathcal{L}}\{\mathbf{u}(t), p(t)\} \stackrel{\text{def}}{=} \mathrm{Re}\sum_{k=1}^{N}\frac{\langle\{\mathbf{u}(t), p(t)\}, \Psi_k(t)\rangle}{||\Psi_k(t)||^2}\Psi_k(t), \quad (6)$$

where $\Psi_k(t) = \eta_k(t) + i\hat{\mathcal{H}}\eta_k(t)$ and $\langle\eta_k(t), \eta_l(t)\rangle \propto \delta_{kl}$. The estimates for $\{\tilde{\mathbf{u}}, \tilde{p}\}$ from $\hat{\mathcal{L}}$ were found to closely reproduce the estimates from $\hat{\mathcal{N}}$.

The phase difference between the wave-coherent air pressure fluctuations on the surface $\tilde{p}(t)$ and the surface elevation signal $\eta(t)$ plays a major role in controlling wind-wave energy exchange. Intuitively, if the maxima of $\tilde{p}(t)$ are behind the maxima of $\eta(t)$ (air pressure fluctuations lagging the wave) wave growth occurs. If the pressure is leading (higher pressure before the wave crests), the waves decay. Therefore, defining and estimating the phase shift between $\tilde{p}(t)$ and $\eta(t)$ brings essential information about the air flow structure and wind-wave energy exchange. Let $\tilde{\mathbf{u}}(t) \equiv (\tilde{u}(t), \tilde{v}(t), \tilde{w}(t))$ be approximated by $[\tilde{u}_0\cos(\Phi(t) + \overline{\varphi}_{\tilde{u}}),\ \tilde{v}_0\cos(\Phi(t) + \overline{\varphi}_{\tilde{v}}),\ \tilde{w}_0\cos(\Phi(t) + \overline{\varphi}_{\tilde{w}})]$, the wave-coherent air pressure fluctuations on the interface $\tilde{p}(t)$ by $\tilde{p}_0\cos[\Phi(t) + \overline{\varphi}_{\tilde{p}}]$, and the surface elevation $\eta(t)$ by $\eta_0\cos\Phi(t)$. Then the vertical flux of horizontal wave-coherent momentum $\tilde{\tau} \stackrel{\text{def}}{=} \langle\tilde{u}(t)\,\tilde{w}(t)\rangle\mathbf{i} + \langle\tilde{v}(t)\,\tilde{w}(t)\rangle\mathbf{j}$ is

$$\tilde{\boldsymbol{\tau}} \simeq (\tilde{w}_0/2)[\tilde{u}_0\cos(\overline{\varphi}_{\tilde{u}} - \overline{\varphi}_{\tilde{w}})\mathbf{i} + \tilde{v}_0\cos(\overline{\varphi}_{\tilde{v}} - \overline{\varphi}_{\tilde{w}})\mathbf{j}], \quad (7)$$

and the energy flux is

$$\left\langle\tilde{p}(t)\frac{\partial\eta(t)}{\partial t}\right\rangle \simeq \frac{1}{2}\omega\,\eta_0\tilde{p}_0\sin(\overline{\varphi}_{\tilde{p}}), \quad (8)$$

where ω is such that $\omega T = \varphi(T) - \varphi(0)$ is the unwrapped wave phase accumulated during the time interval $[0, T]$. Equations (7) and (8) demonstrate the role of the phase differences in controlling the direction of the momentum and energy fluxes. The factor ω in (8) shows that the higher frequency waves are favored for energy exchange. Negative fluxes correspond to momentum or energy being transferred from wind to waves; positive fluxes mean waves-to-wind transfer.

The instantaneous phase difference $\varphi_{\eta\tilde{p}}$ between $\tilde{p}(t)$ and $\eta(t)$ and the mean phase difference $\overline{\varphi}_{\tilde{p}}$ can be defined as

$$\varphi_{\eta\tilde{p}}(t) \stackrel{\text{def}}{=} \arg\frac{\tilde{p}(t) + i\hat{\mathcal{H}}\tilde{p}(t)}{\eta(t) + i\hat{\mathcal{H}}\eta(t)}, \quad (9)$$

$$\overline{\varphi}_{\tilde{p}} \stackrel{\text{def}}{=} -\arctan\frac{\langle\tilde{p}(t), \hat{\mathcal{H}}\eta(t)\rangle}{\langle\tilde{p}(t), \eta(t)\rangle}, \quad (10)$$

respectively. The phase shift between the wave-coherent components in the air flow and the wave has been predicted to occur from the air flow separation (the mean-flow stream lines forming a cat's eye pattern [8,10]), and can be detected and estimated by (9) and (10) from open-ocean experimental data. For example $\overline{\varphi}_{\tilde{u}} = 168°$ from the data in Fig. 1.

Figure 2 shows $\overline{\varphi}_{\tilde{p}}$ vs U_{10}/C_p, where C_p is the phase speed of the most energetic wave component and U_{10} is the mean wind speed at 10 meters from the interface. According to (8), Fig. 2 indicates that the efficiency of the wind-to-wave energy transfer increases with U_{10}/C_p. The pressure sensors were positioned 4 and 12 m above the mean ocean surface. The signal distortion due to the pressure sensor response is considered negligible in the range of time scales of interest [16].

The co-spectrum $Co_{\tilde{u}\tilde{w}}$ of the wave-coherent streamwise $\tilde{u}$ and vertical $\tilde{w}$ velocities represents the wave-coherent momentum flux $\langle\tilde{u}\tilde{w}\rangle$, while $Co_{u'w'}$ represents the turbulent momentum flux $\langle u'w'\rangle$ per unit of time

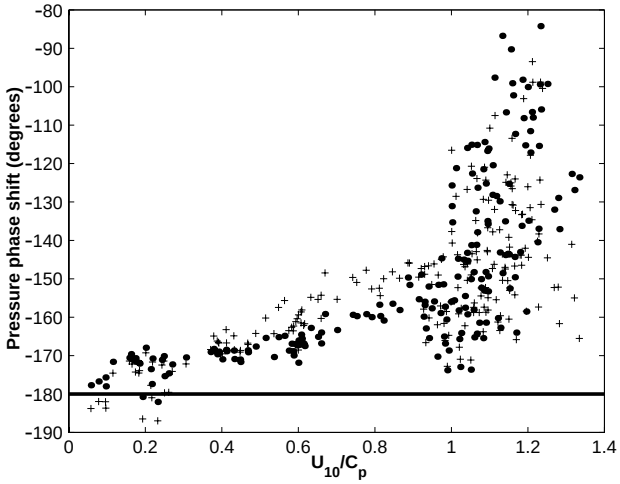

FIG. 2. Phase shift $\overline{\varphi}_{\tilde{p}}$ of the wave-coherent pressure fluctuations vs U_{10}/C_p from 2 sensors: (•) – 4 m and (+) – 12 m from the surface. Each point is obtained by applying (10) to 30 min of data. Should be interpreted according to Eq. (8). The pressure configuration corresponds to wind-to-wave energy transfer ($\overline{\varphi}_{\tilde{p}} > -180°$), except for few cases in the range $0 < U_{10}/C_p \leq 0.3$.

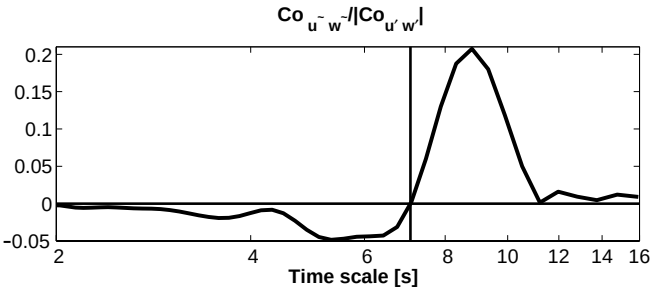

FIG. 3. A representative ratio of the cospectra $Co_{\tilde{u}\tilde{w}}/|Co_{u'w'}|$ vs the time scale. The vertical line at time scale $T_{\overline{u}} = (2\pi/g)\overline{u}$ corresponds to the period of the wave which has a phase speed C_p equal to the mean wind speed $\overline{u}$.

scale. A representative ratio $Co_{\tilde{u}\tilde{w}}/|Co_{u'w'}|$ is shown in Fig. 3 vs time scales. From the dispersion of deep-water waves $\omega^2 = gk$ (g is the acceleration of gravity), we obtain $T_{\overline{u}} = (2\pi/g)\overline{u}$ as the period of the wave mode with phase velocity equal to the mean wind speed $\overline{u}$. $T_{\overline{u}}$, presented as a vertical line on Fig. 3, separates the time scales into periods of wave modes with phase velocities slower than the wind and faster than the wind. For the time scales corresponding to waves slower than the wind, the momentum flux is mostly negative (from wind to waves). For those corresponding to waves faster than the wind, momentum flux is positive (from waves to the wind). Since the wave-coherent fields decay with distance from the interface $|z|$ roughly as $\{\tilde{\mathbf{u}}, \tilde{p}\} \propto Ae^{-k|z|}$ (A is the wave amplitude, k is the wave number), the short-wave effects decay faster with $|z|$. This lowers the intensity of the high-frequency (short wave) part of the co-spectrum (relevant when interpreting Fig. 3). The wind velocity sensor was at $kz = 0.28$ above the mean interface. Sensors positioned higher detect only the positive peak because of the faster exponential decay of the short waves' signature in the air flow.

The data, processed with the technique described above, showed that the absolute value of wave-coherent stress fraction $|\langle\tilde{u}\tilde{w}\rangle/\langle u'w'\rangle|$ can be less than 0.01 for saturated seas (wind-wave interaction is present, but positive and negative parts of $Co_{\tilde{u}\tilde{w}}$ virtually cancel). Also, that absolute value can exceed 0.5 for decaying seas, where preexisting waves are faster than the wind and the shear driven turbulence has low intensity.

In conclusion, we have developed a robust approach to identify cooperative behavior in the wind-wave system by extracting the unobservable wave-coherent component $\{\tilde{\mathbf{u}}, \tilde{p}\}$ in the wind. The detected $\{\tilde{\mathbf{u}}, \tilde{p}\}$ indicates that the resonant interaction mechanism, similar to the one in [3], is active for the long waves. However, addressing the issue of wave generation requires measurements closer to the surface (since $\{\tilde{\mathbf{u}}, \tilde{p}\} \propto Ae^{-k|z|}$) to capture the fluctuations induced by the shortest waves (wavelength $\lambda \leq 1$ m), expected to have major significance for the wave growth. The phase shifts of the wave-coherent fields, resulting from the air flow separation and controlling the wind-wave coupling, were defined and obtained. The wave-coherent stress spectrum was calculated, suggesting that waves grow or decay due to the interaction with the air flow depending on the ratio $C_p/\overline{u}$. The method clearly showed momentum transfer from waves to wind for decaying seas—phenomenon predicted by models, but not heretofore observed in an open ocean experiment.

The work was supported by ONR under Grant No. N00014-93-I-0923. The authors thank the crew of FLIP and the Marine Physical Laboratory for their assistance. The help from especially Jim Edson (experiment), Lloyd Green (wave wire), and Jim Wilczak (pressure sensors) is gratefully acknowledged.

*Email address: tshristo@uci.edu

[1] F. Dobson and B. Toulany, in *Directional Ocean Wave Spectra* (Johns Hopkins University Press, Baltimore, 1991), pp. 22–33.
[2] H. Jeffreys, Proc. R. Soc. London A **107**, 189 (1924).
[3] J. W. Miles, J. Fluid Mech. **3**, 185 (1957).
[4] O. M. Phillips, J. Fluid Mech. **2**, 417 (1957).
[5] D. Chalikov and V. Makin, Bound.-Layer Meteorol. **56**, 83 (1991).
[6] S. Belcher and J. C. R. Hunt, J. Fluid Mech. **251**, 109 (1993).
[7] P. Janssen, in *Dynamics and Modelling of Ocean Waves* (Cambridge University Press, Cambridge, 1994), Chap. II, pp. 71–75.
[8] C. Hsu, E. Hsu, and R. Street, J. Fluid Mech. **105**, 87 (1981).
[9] M. Donelan, in *The Sea* (John Wiley & Sons, Inc., New York, 1990), Vol. 9, pp. 239–292.
[10] M. J. Lighthill, J. Fluid Mech. **14**, 385 (1962).
[11] M. S. Vieira, A. J. Lichtenberg, and M. A. Lieberman, Phys. Rev. A **46**, R7359 (1992).
[12] L. Hasse and F. Dobson, *Introductory Physics of the Atmosphere and Ocean* (D. Reidel Publishing Company, Boston, 1986), pp. 98–114.
[13] O. M. Phillips, *The Dynamics of the Upper Ocean* (Cambridge University Press, Cambridge, 1977), pp. 107–108.
[14] W. Gardner, *Statistical Spectral Analysis, a Nonprobabilistic Theory* (Prentice Hall, Englewood Cliffs, NJ, 1988), pp. 98–102.
[15] A. H. Jazwinski, *Stochastic Processes and Filtering Theory* (Academic Press, New York, 1970).
[16] J. Wilczak (private communication).